Optical analysis of nanoparticles via enhanced backscattering facilitated by 3-D photonic nanojets

Xu Li

Department of Biomedical Engineering, Northwestern University, Evanston, Illinois 60208
xuli@northwestern.edu

Zhigang Chen and Allen Taflove

Department of Electrical and Computer Engineering, Northwestern University, Evanston, Illinois 60208

Vadim Backman

Department of Biomedical Engineering, Northwestern University, Evanston, Illinois 60208

Abstract: We report the phenomenon of ultra-enhanced backscattering of visible light by nanoparticles facilitated by the 3-D photonic nanojet – a sub-diffraction light beam appearing at the shadow side of a plane-wave-illuminated dielectric microsphere. Our rigorous numerical simulations show that backscattering intensity of nanoparticles can be enhanced up to eight orders of magnitude when locating in the nanojet. As a result, the enhanced backscattering from a nanoparticle with diameter on the order of 10 nm is well above the background signal generated by the dielectric microsphere itself. We also report that nanojet-enhanced backscattering is extremely sensitive to the size of the nanoparticle, permitting in principle resolving sub-nanometer size differences using visible light. Finally, we show how the position of a nanoparticle could be determined with subdiffractional accuracy by recording the angular distribution of the backscattered light. These properties of photonic nanojets promise to make this phenomenon a useful tool for optically detecting, differentiating, and sorting nanoparticles.

References and links

1. L. E. Helseth and T. M. Fischer, "Cooperative microlenses," Opt. Express **12**, 3428-3435 (2004). http://www.opticsexpress.org/abstract.cfm?URI=OPEX-12-15-3428
2. M. Mosbacher, H. J. Munzer, J. Zimmermann, J. Solis, J. Boneberg, and P. Leiderer, "Optical field enhancement effects in laser-assisted particle removal," Appl. Phys. A **72**, 41-44 (2001).
3. D. A. Fletcher, K. E. Goodson, and G. S. Kino, "Focusing in microlenses close to a wavelength in diameter," Opt. Letters **26**, 399-401 (2001).
4. Z. Chen, A. Taflove, and V. Backman, "Photonic nanojet enhancement of backscattering of light by nanoparticles: a potential novel visible-light ultramicroscopy technique," Opt. Express **12**, 1214-1220 (2004). http://www.opticsexpress.org/abstract.cfm?URI=OPEX-12-7-1214
5. P. Chylek, J. D. Pendleton, and R. G. Pinnick, "Internal and near-surface scattered field of a spherical-particle at resonant conditions," Appl. Opt. **24**, 3940-3942 (1985).
6. D. S. Benincasa, P. W. Barber, J. Z. Zhang, W. F. Hsieh, and R. K. Chang, "Spatial-distribution of the internal and near-field intensities of large cylindrical and spherical scatterers," Appl. Opt. **26**, 1348-1356 (1987).
7. C. F. Bohren and D. R. Huffman, *Absorption and Scattering of Light by Small Particles* (Wiley, New York, 1983).
8. R. T. Wang and H. C. van de Hulst, " Rainbows: Mie computations and the Airy approximation," Appl. Opt. **30**, 106-117 (1991).
9. C. Liang and Y. T. Lo, "Scattering by 2 Spheres," Radio Sci. **2**, 1481-& (1967).

10. Y. L. Xu and R. T. Wang, "Electromagnetic scattering by an aggregate of spheres: Theoretical and experimental study of the amplitude scattering matrix," Phys. Rev. E **58**, 3931-3948 (1998).
11. http://www.astro.ufl.edu/~xu/
12. P.B. Johnson, R.W. Christy, "Optical constants of the noble metals," Phys. Rev. B **6**, 4370-4379 (1972).
13. V. Backman, V. Gopal, M. Kalashnikov, K. Badizadegan, R. Gurjar, A. Wax, I. Georgakoudi, M. Mueller, C. W. Boone, R. R. Dasari, and M. S. Feld, "Measuring cellular structure at submicrometer scale with light scattering spectroscopy," IEEE J. Sel. Top. Quantum Electron. **7**, 887-893 (2001).

1. Introduction

The effect of enhanced and subdiffractional focus of visible light by dielectric microspheres and microcylinders has been recently brought into attention by a number of researchers through a combination of experimental observations [1, 2], theoretical analysis [1, 3], and numerical calculations [3, 4]. Conventionally, spherical and cylindrical lenses are analyzed by geometrical optics, or more rigorously, the vector diffraction theory. However, as has been pointed out by Flecher *et al.* [3], when the diameter of the dielectric sphere is reduced to be on the order of the wavelength, the distribution of light intensity close to the surface of the sphere cannot be analyzed by the diffraction theory.

Most recently, we have conducted 2-D high-resolution finite-difference-time-domain (FDTD) simulations on plane wave incident on dielectric cylinders [4]. By optimally choosing the size and refractive index of the dielectric microcylinder, we demonstrated the optical phenomenon of photonic nanojet – a localized, subdiffractional, nonevanescent light focus propagating along the line of incidence at the shadow side of the dielectric cylinder. Our 2-D numerical study also demonstrated a remarkable property of photonic nanojets – they can significantly enhance the backscattering of light by nanometer-scale particles located within the jets.

In this paper, we extend our rigorous 2-D numerical study into 3-D to investigate the properties of photonic nanojets created by dielectric microspheres. We demonstrate that, both the intensity and backscattering enhancement capability of the 3-D nanojets are orders of magnitude higher compared to the 2-D cases. As a result, the enhanced backscattering from a nanoparticle with diameter on the order of 10 nm is well above the background signal generated by the dielectric microsphere itself.

In addition, we discuss some practical issues of photonic nanojets to characterize nanoparticles. Specifically, we analyzed the dynamic range requirement, sensitivity of the enhanced backscattering to the size of nanoparticles, and possible approaches to determine the relative position of the nanoparticle in respect to the photonic nanojet. The purpose of these numerical studies is to provide insight into the feasibility of experimentally applying photonic nanojet for characterizing nanostructures.

2. Photonic nanojets generated by dielectric microspheres

First we demonstrate the phenomenon of photonic nanojet in 3-D. By way of background, there have been several calculations reported in the literature for the internal and near-external electromagnetic fields of a dielectric sphere illuminated by a single plane wave [5, 6]. For the case of visible light, calculations of this type have shown a localized micron-scale enhancement of the sphere's external near-field along the line of incidence at the shadow side. While this enhancement exists independent of the resonant condition, its precise distribution and intensity depends upon the size parameter of the sphere and the refractive index contrast between the sphere and its surrounding medium.

Our calculations presented in this section are based on rigorous exact separation-of-variables eigenfunction solution for Maxwell's equations in spherical coordinates. By expanding an incident plane wave of unity amplitude in spherical harmonics as:

$$\mathbf{E}_{inc}(\mathbf{r}) = \sum_{n=1}^{\infty} i^n \{(2n+1)/[n(n+1)]\}[\mathbf{M}_{o1n}^{(1)}(\mathbf{r}) - i\mathbf{N}_{e1n}^{(1)}(\mathbf{r})] \tag{1}$$

where **M** and **N** are the vector spherical harmonics. The expansion for the scattered field, valid for all points outside of the sphere, is given by [7]:

$$\mathbf{E}_{scat}(\mathbf{r}) = \sum_{n=1}^{\infty} i^n \{(2n+1)/[n(n+1)]\}[ia_n \mathbf{N}_{e1n}^{(3)}(\mathbf{r}) - b_n \mathbf{M}_{o1n}^{(3)}(\mathbf{r})] \tag{2}$$

where a_n and b_n are the scattering coefficients and the superscripts appended to **M** and **N** denote the kind of spherical Bessel function. Then, the total external electric field induced by the plane wave is given by $\mathbf{E}_{inc}(\mathbf{r}) + \mathbf{E}_{scat}(\mathbf{r})$. We note that this type of calculation is within the domain of Lorentz-Mie theory, where calculations of far-field scattering properties of spheres are more routinely performed.
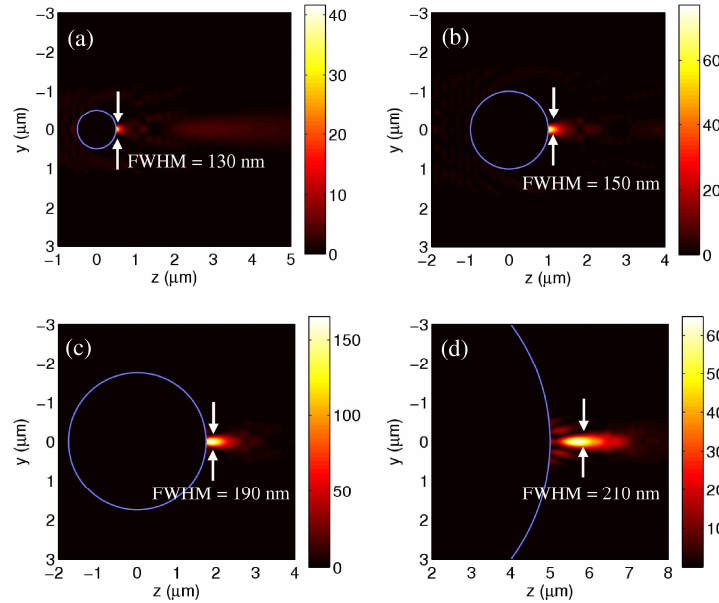

Fig. 1. Photonic nanojets generated by illuminating dielectric spheres ($n_\mu = 1.59$) with a $\lambda = 400\,nm$, $\hat{x}$ - polarized, $\hat{z}$ - propagating incident plane wave in vacuum. The near-field intensity distributions are calculated with Eq. (2). (a) Sphere diameter $D = 1\,\mu m$. (b) $D = 2\,\mu m$. (c) $D = 3.5\,\mu m$. (d) $D = 8\,\mu m$.

We have followed the algorithm described in Ref. [8] to calculate the Mie coefficients a_n 's and b_n 's. Subsequently, we calculate the external near-field distribution using (2) for a series of dielectric spheres. Figure 1 shows the calculated external light intensity distribution resulting from illuminating dielectric spheres with $n_\mu = 1.59$ with an $\hat{x}$ - polarized, $\hat{z}$ - propagating plane wave with unit intensity and wavelength $\lambda = 400\,nm$. For dielectric spheres with $D < 4\,\mu m$ (Fig. 1 (a)-(c)), a subdiffractional light jet protrudes from the shadow side of the dielectric particle. As the diameter increases, the light jet starts to emerge and move away from the dielectric sphere (Fig. 1 (d)). The maximum intensity and full-width-half-max (FWHM) of the light jet also increase as the size of the dielectric sphere increases. For a microsphere with diameter $D = 3.5\,\mu m$ (Fig. 1 (c)), a tight focus of light (photonic nanojet) scale is created with high peak intensity ($I_{max} \approx 160\,I_0$), subdiffractional waist (FWHM = 190 nm), and propagating in micron scale. We note that the incident

wavelength $\lambda = 400$ nm is chosen as an example. The diameters of the dielectric microspheres and the geometric extent of the photonic nanojets are scalable in respect of the incident wavelength.

3. Photonic nanojet enhanced backscattering from nanoparticles in 3-D

Our previous 2-D numerical study [4] demonstrated a remarkable property of photonic nanojets – they can significantly enhance the backscattering of light by nanometer-scale particles located within the jets. The counterpart numerical investigation in 3-D involves calculating scattering from multiple spheres (both the dielectric microsphere and the nanoparticle). These studies are conducted using the Generalized Multiparticle Mie (GMM) method, which is an extension of Mie theory and provides rigorous analytical solution for light scattering by multiple spheres.

The GMM method is based on the addition theorems for vector spherical wave function, as well as the long history of the development of rigorous multiparticle scattering solutions pioneered by Liang and Lo [9]. The underlying theory and a complete computer code have been developed, implemented, and experimentally validated by Xu *et al* [10, 11]. This framework fully accounts for the cooperative scattering effect of arbitrary configurations of multiple spherical particles and therefore, provides us an efficient methodology for calculating the interaction between the scattered fields of the dielectric microsphere and the nanoparticle.
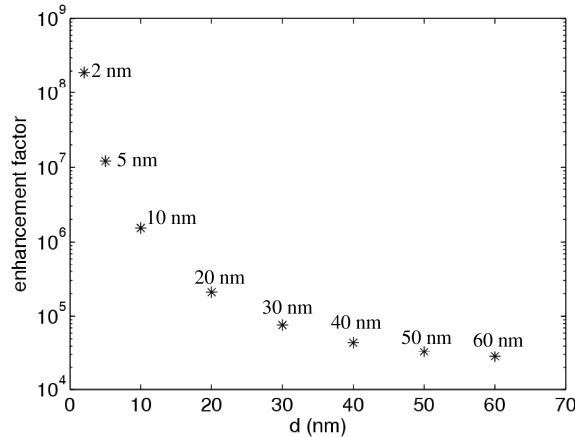

Fig. 2. The backscattering enhancement factor E for a gold nanoparticle placed in the photonic nanojet elevates by orders of magnitude as the nanoparticle size drops below 60 nm. The nanojet is generated by illuminating the $n_\mu = 1.59$, $D = 3.5\,\mu$m dielectric microsphere with plane wave of $\lambda = 400$ nm. The gold nanoparticles are assumed to have refractive index $n_\nu = 1.47 - j1.95$.

Similarly to our previous 2-D numerical studies, we first investigate the enhancement factors of the backscattering from nanoparticles when they are located within photonic nanojet. Using the GMM method, we first calculate the backscattering intensity of the two-sphere system where a nanoparticle is placed in the vicinity of the shadow side of the dielectric microsphere, where the photonic nanojet is present. This backscattering intensity is denoted as $I_{\mu+\nu}$. We also calculate the backscattering intensity for the microsphere alone, I_μ, and the nanoparticle alone, I_ν. The enhancement factor is defined as the change of the backscattering intensity when the nanoparticle is introduced into the nanojet, normalized by the scattering intensity by the nanoparticle alone:

$$E \equiv \delta I/I_\nu = (I_{\mu+\nu} - I_\mu)/I_\nu \qquad (3)$$

Figure 2 graphs the backscattering enhancement factors as a function of the size of the gold nanoparticle ($n_\nu = 1.47 - j1.95$, see Ref. [12]) placed in the nanojet generated by illuminating a 3.5 μm dielectric microsphere ($n_\mu = 1.59$) with a $\lambda = 400$ nm incident wavelength. For nanoparticles of all sizes, the center of the nanoparticle is assumed to be located 240 nm away from the back surface of the microsphere. It is apparent from Fig. 2 that the backscattering intensity of the nanoparticle is dramatically enhanced by the photonic nanojet. Compared to the 2-D cases, the enhancement factors are increased by one to two orders of magnitude.

4. Dynamic range requirements for nanoparticle detection

In addition to the enhancement factor, the normalized backscattering intensity perturbation,

$$\Delta I_N \equiv \delta I / I_\mu = (I_{\mu+\nu} - I_\mu) / I_\mu , \tag{4}$$

is another important parameter characterizing the backscattering enhancement effect of the photonic nanojet. In contrast with the definition for enhancement factor E given in Eq. (1), ΔI_N is defined as the intensity perturbation δI normalized by the backscattering intensity of the isolated microsphere I_μ , instead of I_ν . The significance of this parameter is explained as the following. Note that the perturbation signal, δI , which results from introducing the nanoparticle into the photonic nanojet, is measured on top of the background signal I_μ . Therefore, normalizing δI by I_μ is directly linked to the dynamic range requirement for the detector to detect and resolve this perturbation.
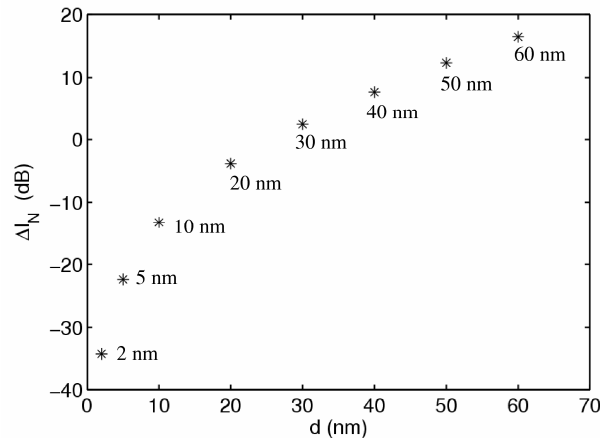

Fig. 3. The normalized backscattering intensity perturbation, defined as $\Delta I_\nu \equiv \delta I / I_\mu$, lies within the range of -35 dB to +15 dB relative to the backscattering intensity of the microsphere for nanoparticles diameters of 2—60 nm. This is within the dynamic range of available optical instruments, implying that nanoparticles as small as a few atoms across could be detected with visible light.

Figure 3 re-plots the data presented in Fig. 2 by replacing the enhancement factor E by the normalized backscattering intensity perturbation ΔI_N in a dB scale. This graph demonstrates the substantial perturbation of the backscattering intensity due to the introduction of the nanoparticle in the photonic nanojet. For example, the intensity perturbation caused by the presence of the nanoparticle with $d = 30$ nm is about two times (~3dB) of the backscattering intensity of the microsphere I_μ . Even for a 5-nm gold nanoparticle, the backscattering perturbation is 0.6% of I_μ (~ -20 dB). This perturbation can

be detected by a commercially available 16-bit CCD detector which provides dynamic range around 50 dB.

The effect of strong perturbation generated by the nanoparticle can be better visualized in Fig. 4. Here, we demonstrate our numerical experiment emulating the experimental configuration where a nanoparticle is moving through the photonic jet while the scattering signals are monitored continuously. As illustrated in Fig. 4(a), a dielectric microsphere ($n_\mu = 1.59$, $D = 3.5\mu m$) is placed at a fixed location with collimated incident light ($\lambda = 400nm$) propagating in the +z direction. A gold nanoparticle ($n_\nu = 1.47 - j1.95$, $d = 20nm$) is positioned in the vicinity of the shadow side of the dielectric microsphere where the photonic nanojet is located. The backscattering intensity of this two-sphere system $I_{\mu+\nu}$ is calculated while varying position of the nanoparticle relative to the microsphere and obtained the scattering intensity as a function of the position. Figure 4(b) plots the normalized backscattering intensity of the two-sphere system $I_{\mu+\nu} / I_\mu$ as the lateral position of the 20-nm gold nanoparticle varies from $-1\mu m$ to $+1\mu m$ with respect to the center of the nanojet. The separation between the back surface of dielectric sphere and the center of the nanoparticle is fixed at 240 nm. It is evident from Fig 4(b) that the 20-nm nanoparticle generates a strong perturbation of the backscattering signal ($\Delta I_N \sim 40\%$) when it flows through the center of the photonic nanojet. This perturbation can be easily detected and characterized by laboratory instruments.
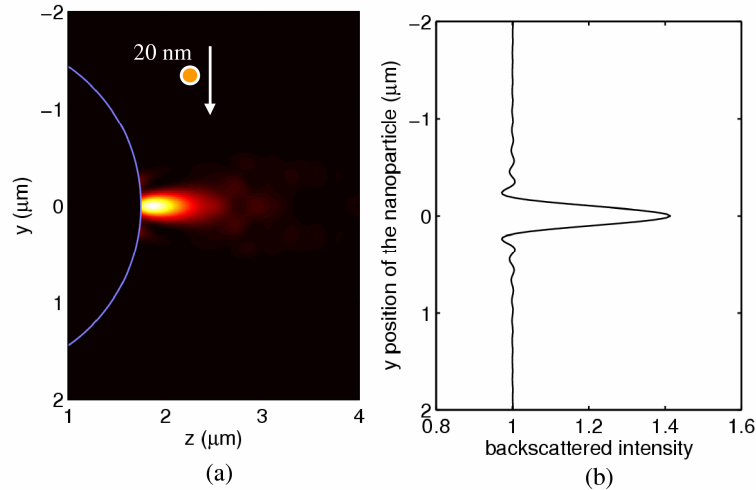

Fig. 4. Simulation of a 20-nm gold nanoparticle moving through a photonic nanojet while the backscattering signal is recorded. (a) Geometry. (b) Normalized backscattering intensity (relative to by the dielectric microsphere alone) as a function of the position of the nanoparticle. We see that the nanoparticle generates a 40% jump in the recorded backscattering signal at its peak response.

5. Sizing and locating nanoparticle using photonic nanojet

One potential application of the significantly enhanced backscattering from nanoparticles located in the photonic nanojets is to characterize their sizes by examining the backscattering perturbation. Figure 5 repeats the numerical experiment presented in Fig. 4 for nanoparticles with slight size variations (with 1-nm increment in diameter) and compares the observed backscattering signals. This comparison demonstrates the extreme sensitivity of the backscattering intensity to the size of the nanoparticle located in the photonic nanojet. As a

practical implication of this effect, the photonic nanojet may provide a straightforward means for resolving the size of a single nanoparticle with 1 nm precision.
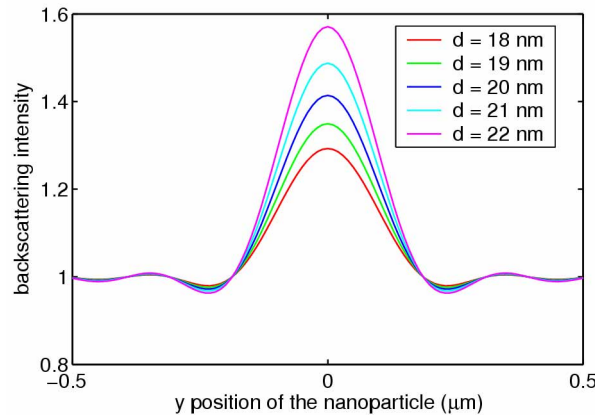

Fig. 5. High sensitivity of the nanoparticle backscattering signal (recorded with configuration shown in Fig. 4 (a)) relative to a nm-size variations of the nanoparticle. These signal perturbations are well within the measurement dynamic range of available laboratory instrumentation.

For practical implementation of nanoparticle sizing based the backscattered intensity, it is desirable to obtain the position of the nanoparticle with respect to the nanojet using additional parameter(s). Here we demonstrate the feasibility of utilizing the angular pattern of the backscattered light to achieve this purpose.

It has been experimentally demonstrated that the angular scattered light distribution vs. the scattering angle θ and azimuth angle φ can be mapped simultaneous by collecting the backscattered light with a lens and project the angular distribution to a CCD array placed at the focal plane on the other side of the lens [13]. To emulate this projection procedure, we calculate backscattering intensity perturbation ΔI_N for an angular range of $\theta = 180° \pm 2°$ and $\varphi = 0° \to 180°$ for the two-sphere system illustrated in Fig. 4(a). Then we map the angular distribution of ΔI_N to a 2-D plane similarly as the projection achieved by the lens in the experimental setup [13]. Figure 6 shows the projected angular distribution of ΔI_N in the polarization parallel to incident light in a dB scale for four relative positions, incident light in a dB scale for four relative positions, $y = -150\,\text{nm}$, $y = -100\,\text{nm}$, $y = -50\,\text{nm}$, and $y = 0$. It is clear from Fig. 6 that a slight off-center displacement (50nm in Fig. 6(c)) of the nanoparticle can generate distinct unsymmetrical pattern in the angular distribution of the backscattered light. In turn, these angular patterns can be used to locate the relative position of the nanoparticle with subdiffractional accuracy.

6. Summary and discussion

In this paper, we reported the phenomenon of ultra-enhanced backscattering of visible light by nanoparticles facilitated by the 3-D photonic nanojet — a sub-diffraction light beam appearing at the shadow side of a plane-wave-illuminated dielectric microsphere. Our rigorous numerical studies showed that the enhancement is so profound that a 30-nm gold particle located within a nanojet could exhibit twice of the backscattering intensity of a dielectric sphere more than 100 times its diameter; and a 5-nm gold particle could exhibit a backscattering only 20 dB below that of a same sphere. We also reported that nanojet-enhanced backscattering is extremely sensitive to the size of the nanoparticle, permitting in principle resolution of sub-nanometer size differences using visible light. Finally, we showed

how the position of a nanoparticle could be determined with subdiffractional accuracy by recording the angular distribution of the backscattered light.

The above properties of photonic nanojets promise to make this phenomenon a useful tool for optically detecting, differentiating, and sorting nanoparticles. By analyzing the intensity and angular distribution of enhanced backscattering from nanoparticles located within the nanojet, one can derive the nanoparticle's size and relative position with nanometer precision. This tool could be of importance in the fields of nanotechnology and nano-biotechnology, including potential applications such as drug delivery via nanoparticles and nanoparticle-assisted molecular tissue imaging, where accurate characterization and selection of nanoparticles are crucial. In addition, we envision that this technique could be utilized for a wide variety of related applications including cell nanoarchitecture analysis and detection of viruses, cell fragments, and macromolecular complexes.
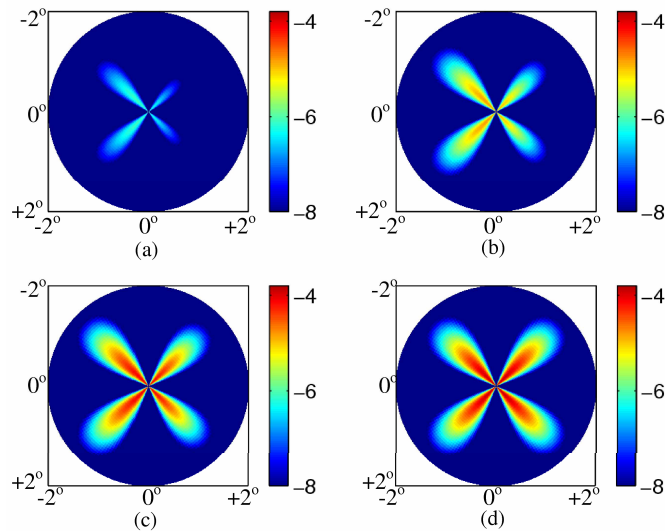
Fig. 6. Angular maps (dB scale) of the normalized co-polarized backscattering intensity perturbation for four positions of a 20-nm gold nanoparticle relative to the center of the nanojet shown in Fig. 4 (a). (a) $y = -150\,\text{nm}$. (b) $y = -100\,\text{nm}$. (c) $y = -50\,\text{nm}$. (d) $y = 0$. We see that a nanoparticle displacement of only 50 nm from the nanojet center is sufficient to noticeably break the symmetry of the angular pattern. Such maps could be used to locate the nanoparticle with subdiffractional precision.

Acknowledgments